LA-13217-MS

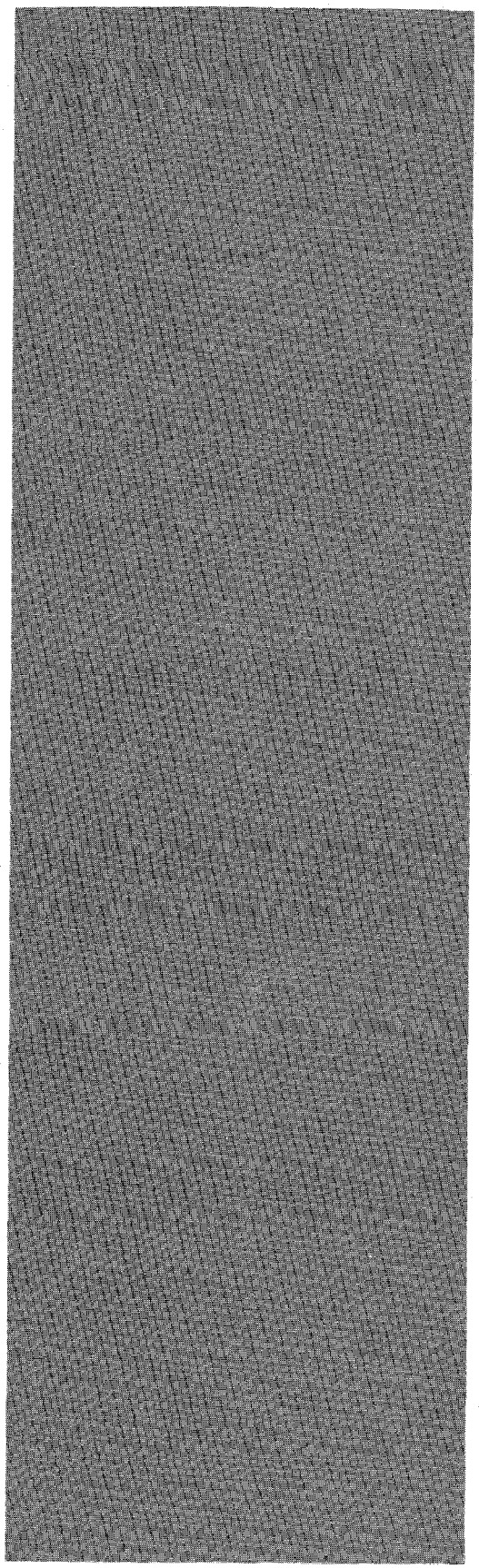

General Features of Hugoniots — II

Los Alamos
NATIONAL LABORATORY

Los Alamos National Laboratory is operated by the University of California for the United States Department of Energy under contract W-7405-ENG-36.

An Affirmative Action/Equal Opportunity Employer

LA-13217-MS

UC-910
Issued: January 1997

General Features of Hugoniots — II

J. D. Johnson

Los Alamos
NATIONAL LABORATORY
Los Alamos, New Mexico 87545

GENERAL FEATURES OF HUGONIOTS—II

by

J. D. Johnson

ABSTRACT

I have derived a differential version of the principal Hugoniot jump relations for a shock wave. From this algebraic equation, relating equation of state and $U_s - U_p$ Hugoniot variables, I explain the general features of the Hugoniot, including two regions of linearity, limiting forms, and insensitivity to shell structure.

Introduction

There has been continuing interest in the behavior of shock Hugoniots for high pressures, in particular for particle velocities greater than $10\ km/s$. Data has been obtained for such mainly through laser and nuclear shock experiments [1-4]. These data, plotted either as shock velocity U_s of a sample material versus U_s of an assumed standard material or as U_s versus the particle velocity U_p of the sample, are remarkably linear. Modeling, as represented by the SESAME database [5], shows the same behavior. A general understanding of this high pressure linearity and of the Hugoniot as a whole is needed.

Formalism

Rather than go to detailed, complex modeling, I use only the Hugoniot jump conditions and thermodynamics to explain the linear regime and all general features of the Hugoniot. I assume that I have the hydrodynamic equation of state $P(\rho, E)$ and the three Hugoniot relations [6]

$$P = \rho_o U_s U_p \ , \tag{1a}$$

$$\rho / \rho_o = U_s / \left(U_s - U_p\right) \ , \tag{1b}$$

and

$$E = \frac{1}{2} U_p^2 . \tag{1c}$$

Here P is pressure, ρ is density, and E is internal energy per gram. Starting from an initial point ρ_o, $P_o = 0$, and $E_o = 0$, and solving $P(\rho, E)$ and Eq. (1c) for $P(\rho)$, one obtains the pressure versus density principal Hugoniot. Then from Eqs. (1a) and (1b) follows the $U_s - U_p$ curve. I instead derive a differential form of the jump conditions. First differentiate Eqs. (1a), (1b), and (1c) with respect to U_p along the Hugoniot, and then express the derivative of P in terms of density and energy derivatives with the use of the partial chain rule. After some algebra and thermodynamic relations, I finally obtain the exact equation

$$B_s / P - x = 3s - 1 + s(2s - 2 - \gamma)/x. \qquad (2)$$

Here, $x = c/U_p$, $\gamma = \frac{1}{\rho}\frac{\partial P}{\partial E}\Big)_\rho$, and $\frac{\rho}{P}\frac{\partial P}{\partial \rho}\Big)_E = B_s/P - \gamma$, where the isentropic bulk modulus is $B_s = \rho\,\frac{\partial P}{\partial \rho}\Big)_s$. The lower case s is the slope of the local tangent line of the $U_s - U_p$ curve at U_p, and c is the $U_p = 0$ intercept of the tangent. All quantities in Eq. (2) are on the Hugoniot and thus are to be thought of as functions of U_p or another Hugoniot variable. This equation is a complex algebraic relation among s, c, U_p, γ, P, and B_s, but it is quite manageable and we can learn from it.

Orientation

Before I give results from the above, let me present the generic behavior of a metal Hugoniot with only phase transitions with small volume change. I use our latest Mo equation of state (solid line in graphs) as an example [5]. The structures will seem small, but this is the reality of $U_s - U_p$ curves. I look at two figures. In Fig. 1 we see the lower Hugoniot which is given very accurately by two dashed straight lines, one with slope 1.245, the other with 1.196. There is clearly a break between them at $U_p \cong 5\ km/s$. This is typical for many materials, as it is usually between 3 and 7 km/s, but the break is a little small because for Mo the lower slope is close to the upper value of 1.196. In other materials, such as in Figs. 3 and 4, the initial slope is larger. Figure 2 shows a larger scale with the same dashed line fit to the upper part of Fig. 1. From $U_p \cong 6\ km/s$ to over 100 km/s, it is an excellent fit. The two chain-dashed lines are straight lines through the origin, the upper with slope 4/3, the lower with slope 1.228. The upper is the ideal gas limit which the physical Hugoniot must ultimately approach. The lower is the lowest slope tangent line to the $U_s - U_p$ curve that goes through the origin. In such a circumstance $c = 0$. Then from Eq. (1b), ρ is not varying, so the density derivative of P is infinite. In my example this point on the Hugoniot is the turnaround point, or point t, and is the maximum

density on the Hugoniot. In the case of Mo, $U_{p,t} \cong 262\ km/s$. For stronger shocks, $c<0$, and the density is decreasing as U_p increases. At any point where $c=0$, P has infinite slope, and, since $x_t=0$, then from Eq. (2), $s_t=1+\gamma_t/2$. Also from Eq. (1b), $\rho_t/\rho_o=s_t/(s_t-1)$. Typically for many materials ρ_t/ρ_o ranges between 5 and 6.2 implying that $1.19 \le s_t \le 1.25$ and $0.38 \le \gamma_t \le 0.5$. The slope of the very linear section between $U_p \cong 10$ and maybe $100\ km/s$ or more ranges between 1.14 and 1.22. Finally, one sees that the approach to the ideal gas line of slope 4/3 is very slow. The Mo Hugoniot is only approaching the ideal gas by $U_p \cong 2000\ km/s$.

Results

Now follows some analysis using my equation. If one takes the $U_p \to 0$ limit of Eq. (2), I obtain the very initial slope and curvature of the Hugoniot as the Taylor series $U_s/c_o=1+s_oU_p/c_o+e\left(U_p/c_o\right)^2....$ (One must in all analysis of the formalism carefully expand all quantities self-consistently.) After a few thermodynamic manipulations, I obtain $s_o=\frac{1}{4}\left[1+\left(\frac{\partial B_s}{\partial P}\right)_S\right]$ and $e=\left[0.5\rho_o\left(\frac{\partial^2 B_s}{\partial\rho\partial P}\right)_S+s_o\left(2+\gamma_o-s_o\right)\right]/6$. The initial slope is directly given by the pressure derivative of the bulk modulus at constant entropy, and the curvature is given by the higher constant entropy derivative of the B_s with γ_o first entering the expansion at this order. It is common, my Mo is an example, that the Hugoniot out to the break is very linear. This form for e partially explains why. The two terms for e are dimensionless quantities and in magnitude should lie between one and ten. The sign of the first is negative, the second positive with resulting cancellation. After dividing by six, one expects e to be small with resulting linear U_s-U_p. For Nb, I estimate that $e=0.16$ [7]. The natural variables that follow from the analysis of Eq. (2) for the series are U_s/c_o and U_p/c_o, where c_o is the bulk sound velocity at $U_p=0$. This implies that the break should occur for $U_p \sim c_o$. We will see later that $U_p=1.6\,c_o$ predicts the break quite well.

One can do large U_p expansions to find the approach to ideal gas. If it is assumed that

Debye-Hückel theory [8] describes the very high temperature gas, for large U_p, $\gamma \sim \frac{2}{3} - b/U_p^3$, $b>0$. Then from Eq. (2), $s \sim \frac{4}{3} + a/U_p^2 - 2b/U_p^3, c \sim -2a/U_p + 3b/U_p^2$, and $P \sim 12\rho_o a/(\rho/\rho_o - 4)$ with $a>0$. The parameter a is given by the sum of cohesive, ionization, and dissociation energies in going from ambient to $T \to \infty$.

I can expand around point t and find the curvature. Letting $U_s = s_t U_p + \alpha_t (U_p - U_{p,t})^2$, α_t is given by $\alpha_t = \gamma_t^{(1)}(1+\gamma_t/2)/(2B_{s,t}/P_t - \gamma_t)$. It is a good approximation that $\alpha_t = \gamma_t^{(1)}/2$. $(\gamma_t^{(1)} \equiv d\gamma/dU_p \text{ at } t.)$ Using numbers from the Mo equation of state, $\alpha_t \sim 10^{-4}\, s/km$, and U_s is well approximated by the quadratic form for $|U_p - U_{p,t}| \lesssim 100\ km/s$.

At this point I already have an argument for the $U_s - U_p$ curve to be very linear for $10 \lesssim U_p \lesssim 200\ km/s$ or even higher. There has to be an inflection point between 10 and 262 km/s. I estimate for Mo from Eq. (2) that it is at $U_p \cong 125\ km/s$. There α is zero and should continue for smaller U_p to be small and negative. (Think of a Taylor series around the inflection point.) Thus the curvature is very small and the curve is close to linear. I actually did not even need to estimate α_t because the slow approach of the $U_p - U_p$ curve to the ideal gas behavior implies it is small.

But I can go into more detail with Eq. (2). For that I need the qualitative behavior of γ and B_s/P as functions of U_p which is obtained from the SESAME database, where the relevant physics comes from either TFD models or the Inferno model [9-10]. The two models are compatible to the level I need, and one can see that the predicted features of γ and B_s/P are physical. At low U_p, γ is high, say 1.5. For U_p between 3 and 7 km/s, for which the temperature is between 10^4 and 3×10^4 K, γ drops fairly rapidly toward 0.4. Once U_p is greater than 7 km/s or so, γ goes through a very broad minimum with $\gamma^{(1)}$ being very small. Ultimately, at large U_p, γ slowly rises to go to the ideal gas limit of 2/3. The physics of the decline of γ is that the electronic thermal excitations are starting to dominate the equation of state at the $U_s - U_p$ break point. They pull γ down below the ideal gas value through the region the electrons are ionizing. For small U_p, B_s/P diverges

as $1/U_p$, but, as U_p increases, B_s/P decreases to $\gamma+1$.

The physics of all this is that for smaller $U_p \lesssim 7$ *km/s* the equation of state is dominated by the zero temperature isotherm and the phonons. Here, to avoid the left-hand side of Eq. (2) being large, c is constrained to be approximately equal to c_o, thus making the $U_s - U_p$ linear. As U_p increases and goes through the break the thermal excitations, the electrons, come into play. The left-hand side of Eq. (2) is now not important, and the $1/x$ term constrains $s \cong 1+\gamma/2$. Thus γ determines s, and the electrons are pulling γ down toward 0.4. All this causes the break. Putting this together in Eq. (2), I have that s is well approximated by $s = 1+\gamma/2$ for U_p from just above the break at $3-7$ *km/s* to well above the turnaround. With $\gamma \cong 0.4$, $s \cong 1.2$ for the region between 10 and 100 *km/s*, quite in line with my earlier statement of between 1.14 and 1.22. Thus the break and high pressure linearity are explained.

Experimental Comparison

All of what I have said fits very well with the detailed modeling that goes into the SESAME database, both TFD and Inferno. It also agrees very well with experiment. Figure 3 shows data for iron and two straight line, least-square fits to the upper and lower portions of the data. I do not show all the lower data, as it then would be too dense; it is very linear with a fitted slope of 1.553. The other line, fitted to the upper five crosses, has a slope of 1.213, in excellent agreement with all I have said. The uppermost cross, one of the pair next down, and the fourth and sixth crosses down are absolute measurements. The x's are data of Ragan [1] with Mo as a standard, and the remaining two high U_p crosses are measured assuming lead as a standard. The error bars on the uppermost point are $\pm 2\%$ in both U_p and U_s. The high U_p crosses and some of the low U_p come from the Russian literature [11]. The rest of the low data points are from the Los Alamos Shock Compendium [12]. I have also looked at Cu, Bi, Sn, Ar, Xe and Al, which all show the break with slopes above it of 1.170, 1.203, 1.162, 1.144, 1.166, and 1.149, respectively [12-14].

These data do not go to as high a U_p as that of the iron, but they do strongly support the existence of the break and the linearity. Figure 3 shows Cu, and Fig. 4 presents Bi, Fe, Cu, Sn, Ar and Xe.

I look now to the break and define it by the intersection of the linear fits to the higher and lower portions of the $U_s - U_p$. In Fig. 5, I plot the location of the break as a function of c_o for Al, Fe, Cu, Sn, Bi, Ar, and Xe, going down from the highest points to the lowest. The solid curve is a fit with a straight line through the origin; the slope is 1.6.

There are data on N_2, a molecular system, which show a break, and also there is a model showing a negative γ in the dissociation region [14, 15]. I am pushing a little to compare here, but the slope above the break is 0.985 and $\gamma = -0.03$. Dissociation pulls the γ down lower than ionization.

Shell Structure

I now discuss the effect of shell structure on the Hugoniot above the break. Here shell structure enters in two ways. One is through the variation in ρ_o in going through the periodic table. This, in particular, varies the location of the turnaround point. But I do not want to focus on this. I look to the shell structure from the thermal part of the equation of state. I obtain upper bounds on the variation of γ and $B_s / P - \gamma$ due to shell structure from Inferno. I see no shell structure in $B_s / P - \gamma$, and, as this is a density derivative, this makes sense. So I drop $B_s / P - \gamma - 1$ from the equations, and I can argue that this is a conservative approximation for the size of the variation in s. For Al and elements with higher atomic numbers, the maximum variation in γ is ± 0.1, with a functional form that is quadratic in $\ln U_p$ and a width guided by Inferno.

From Eq. (2), the variation in s is $\Delta s = \left(\Delta\gamma - \Delta c / U_p\right)/2$, and Δc can be obtained in terms of $\Delta\gamma^{(1)}$. So one finds the variation in s, but what is of interest is ΔU_s which is an integral of Δs. Carrying all this out, I find that for the ± 0.1 in γ, U_s varies by $\pm 2\%$, quite in line with what is seen in full SESAME equations of state based on Inferno. These are

conservative approximations, and this is a maximum variation at an exact U_p. It will be extremely difficult to see shell structure above the break. If one goes to the $P(\rho)$ Hugoniot and looks in the neighborhood of the turnaround, the small wiggles in U_s are amplified by the presence of the singularity and appear large. But experiments are not known that can measure P and ρ directly, so this is not relevant.

Summary

I have presented a number of results. First is Eq. (2), which relates Hugoniot variables and thermodynamic quantities. From it I have expansions of the Hugoniot for $U_p \to 0$, $U_p \to \infty$, and U_p at turnaround. From simple features of the equation of state, the linear region above the break is understood, and the slope and the location of the break are estimated. The perturbation of thermal shell structure is quantified.

I have focused in this paper on elemental metals, and certainly I feel the ideas are valid there. (I am not referring here to the exact results, such as Eq. (2), but to the approximate results.) For all other substances, if one is high enough up the Hugoniot that all molecules are dissociated, then all these ideas should be applicable. Further down, the details of my picture will be altered for molecular systems and insulators. An example here is N_2. Furthermore, below the break where thermal excitations do not dominate, phase transitions with large volume changes introduce structure. Also, for the alkali metals there are shell structure effects for small U_p. But even with these caveats, I have a very powerful overview.

Acknowledgement

I wish to thank all my friends, from minor acquaintances to those closest to me, for putting up with me through this project. This work was supported by the U.S. Department of Energy under contract number W-7405-ENG-36.

References

(1) C. E. Ragan III, Phys. Rev. A 29 (1984) 1391, and references therein.

(2) W. J. Nellis, J. A. Moriarty, A. C. Mitchell, M. Ross, R. G. Dandrea, N. W. Ashcroft, N. C. Holmes and G. R. Gathers, Phys. Rev. Lett. 60 (1988) 1414.

(3) R. Cauble, D. W. Phillion, T. J. Hoover, N. C. Holmes, J. D. Kilkenny and R. W. Lee, Phys. Rev. Lett. 70 (1993) 2102.

(4) M. Koenig, B. Faral, J. M. Boudenne, D. Batani, A. Benuzzi, S. Bossi, C. Rémond, J. P. Perrine, M. Temporal and S. Atzeni, Phys. Rev. Lett. 74 (1995) 2260.

(5) S. P. Lyon and J. D. Johnson, Sesame: Los Alamos National Laboratory Equation of State Database, Los Alamos report no. LA-UR-92-3407, 1992 (unpublished).

(6) See, for example, J. O. Hirschfelder, C. F. Curtiss and R. B. Bird, *Molecular Theory of Gases and Liquids* (John Wiley and Sons, Inc., New York, 1954).

(7) I thank J. Wills for furnishing me with an estimate of the double derivative of B_s for Nb.

(8) L. D. Landau and E. M. Lifshitz, *Statistical Physics* (Addison-Wesley Publishing Company, Reading, PA, 1969).

(9) R. D. Cowan and J. Ashkin, Phys. Rev. 105 (1957) 144.

(10) D. A. Liberman, Phys. Rev. B 20 (1979) 4981.

(11) L. V. Al'tshuler, A. A. Bakanova, I. P. Dudoladov, E. A. Dynin, R. F. Trunin and B. S. Chekin, J. Appl. Mech. Techn. Phys. 22 (1981) 145; L. V. Al'tshuler and B. S. Chekin, in: Proceedings of First All-Union Pulsed Pressure Symposium, VNIIFTRI, Moscow, 1974 (unpublished); L. V. Al'tshuler, N. N. Kalitkin, L. V. Kuz'mina and B. S. Chekin, Sov. Phys.-JETP 45 (1977) 167; R. F. Trunin, M. A. Produrets, L. V. Popov, V. N. Zubarev, A. A. Bakanova, V. M. Ktitorov, A. G. Sevast'yanov, G. V. Simakov and I. P. Dudoladov, Sov. Phys.-JETP 75 (1992) 777; R. F. Trunin, M. A. Podurets, B. N. Moiseev, G. V. Simakov and A. G. Sevast'yanov, Sov. Phys.-JETP 76 (1993) 1095; and references therein.

(12) S. P. Marsh, Ed., *LASL Shock Hugoniot Data* (University of California Press, Berkeley, 1980).

(13) See Ref. 11. Also, S. B. Kormer, A. I. Funtikov, V. D. Ulrin and A. N. Kolesnikova, Sov. Phys.-JETP 15 (1962) 477; B. L. Glushak, A. P. Zharkov, M. V. Zhernokletov, V. Ya. Ternovoi, A. S. Filimonov and V. E. Fortov, Sov. Phys.-JETP 69 (1989) 739; M. V. Zhernokletov, V. N. Zubarev and Yu. N. Sutulov, Zh. Prikl. Mekh. Tekhn. Fiz. 1 (1984) 119; L. P. Volkov, N. P. Voloshin, A. S. Vladimirov, V. N. Nogin and V. A. Simonenko, Sov. Phys.-

JETP Lett. 31 (1980) 588; V. A. Simonenko, N. P. Voloshin, A. S. Vladimirov, A. P. Nagibin, V. P. Nogin, V. A. Popov, V. A. Sal'nikov and Yu. A. Shoidin, Sov. Phys.-JETP 61 (1985) 869; and E. N. Avrorin, B. K. Vodolaga, N. P. Voloshin, V. F. Kuropatenko, G. V. Kovalenko, V. A. Simonenko and B. T. Chernovolyuk, Sov. Phys.-JETP Lett. 43 (1986) 308.

(14) W. J. Nellis and A. C. Mitchell, J. Chem. Phys. 73 (1980) 6137 and W. J. Nellis, M. van Thiel and A. C. Mitchell, Phys. Rev. Lett. 48 (1982) 816.

(15) W. J. Nellis, H. B. Radousky, D. C. Hamilton, A. C. Mitchell, N. C. Holmes, K. B. Christiansen and M. van Thiel, J. Chem. Phys. 94 (1991) 2244 and H. B. Radousky, W. J. Nellis, M. Ross, D. C. Hamilton and A. C. Mitchell, Phys. Rev. Lett. 57 (1986) 2419.

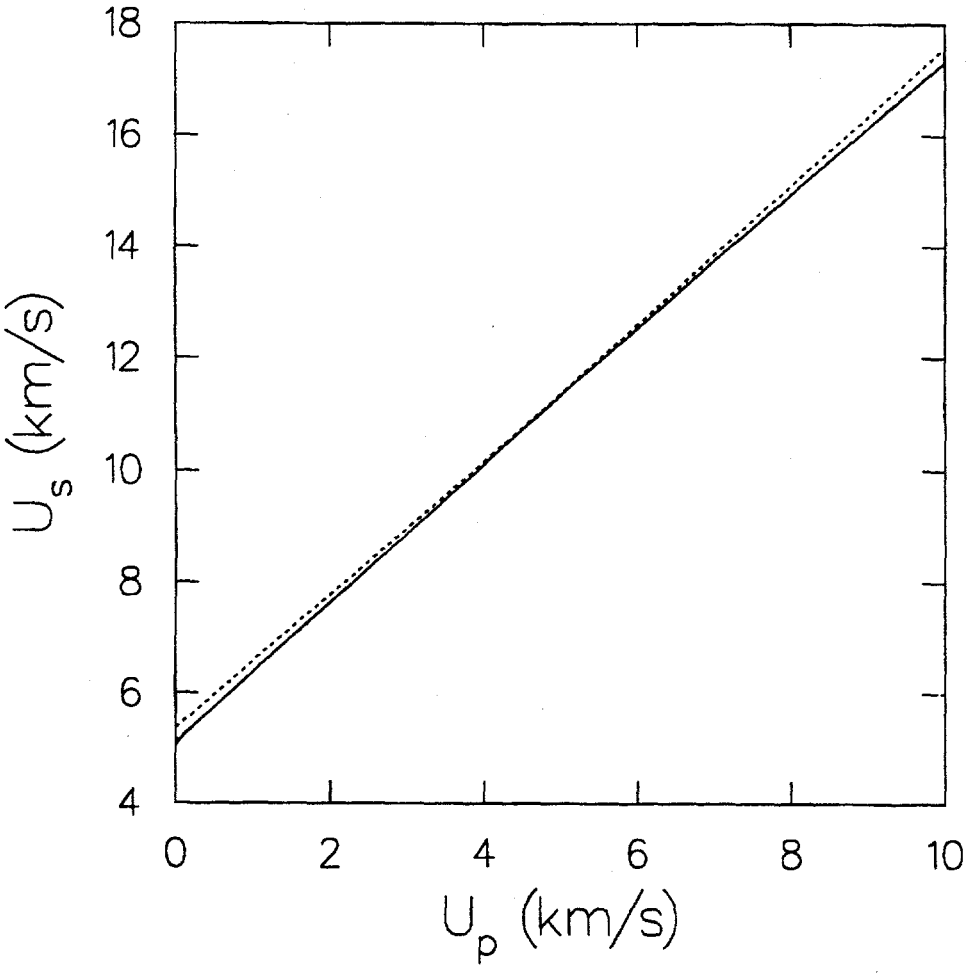

Fig. 1. Mo Hugoniot—lower portion around break. The solid line is the Mo Hugoniot. The two dashed lines are straight line fits to the two linear portions of the Hugoniot. (The dashed lines might appear to the eye as one straight line since their slopes are almost the same. Their intersection is around $5\ km/s$.)

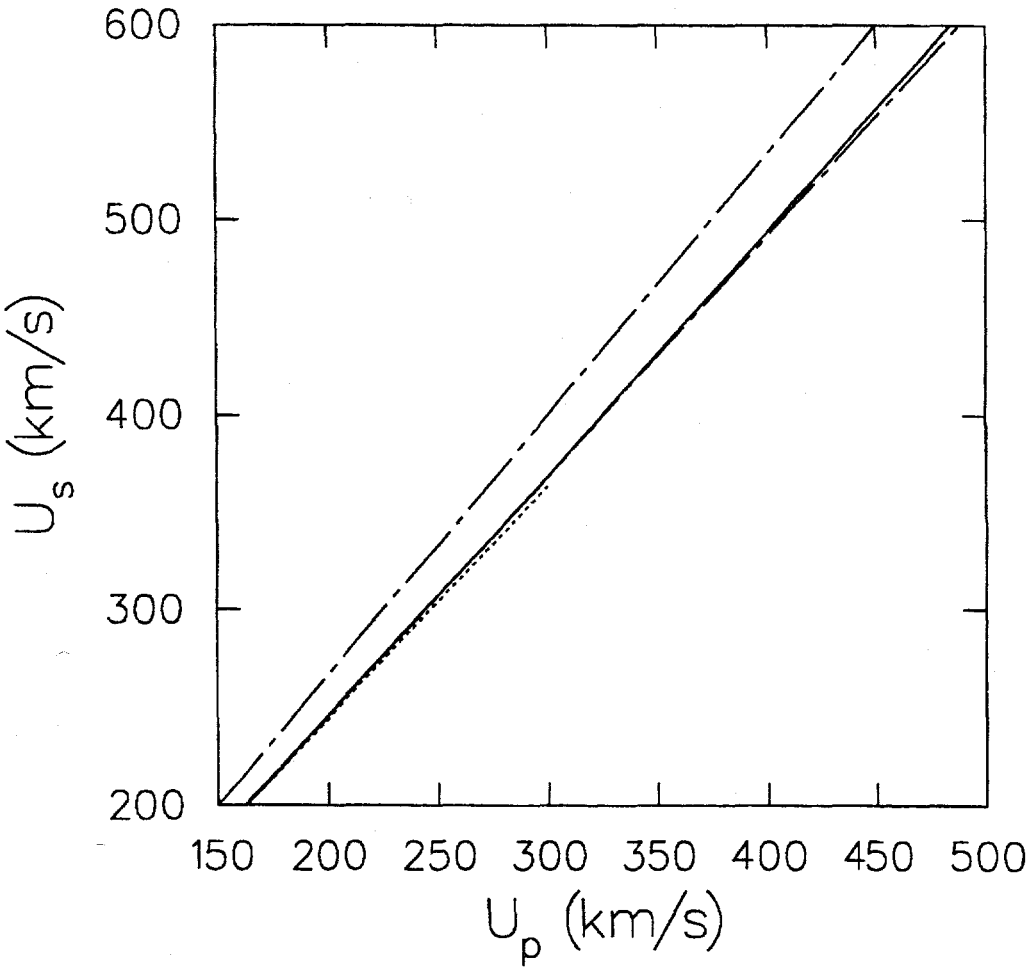

Fig. 2. Mo Hugoniot— U_p out through turnaround. The dashed line is from the fit above the break. It shows that the straightness of the solid Hugoniot curve persists to quite high U_p.

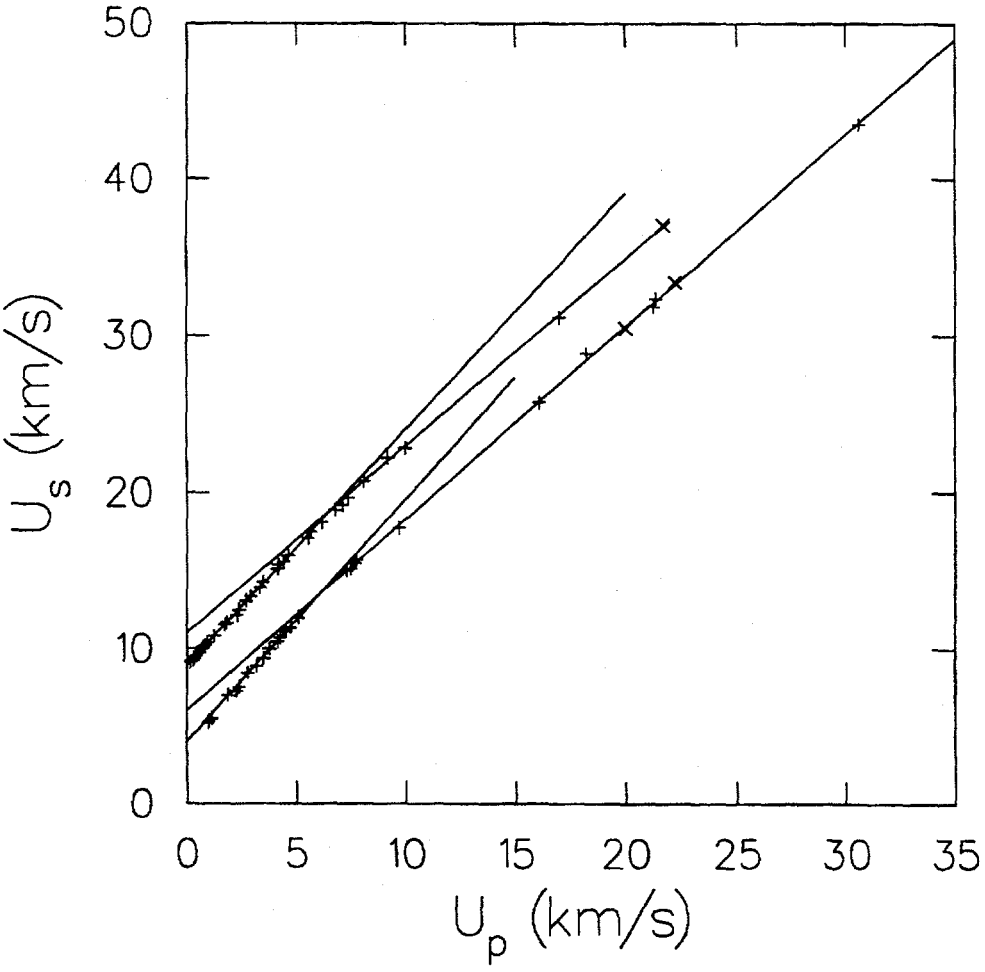

Fig. 3. Fe and Cu Hugoniot data. We see clearly the linearity of the upper data and a well-defined break. The Cu data and curves have been shifted upwards.

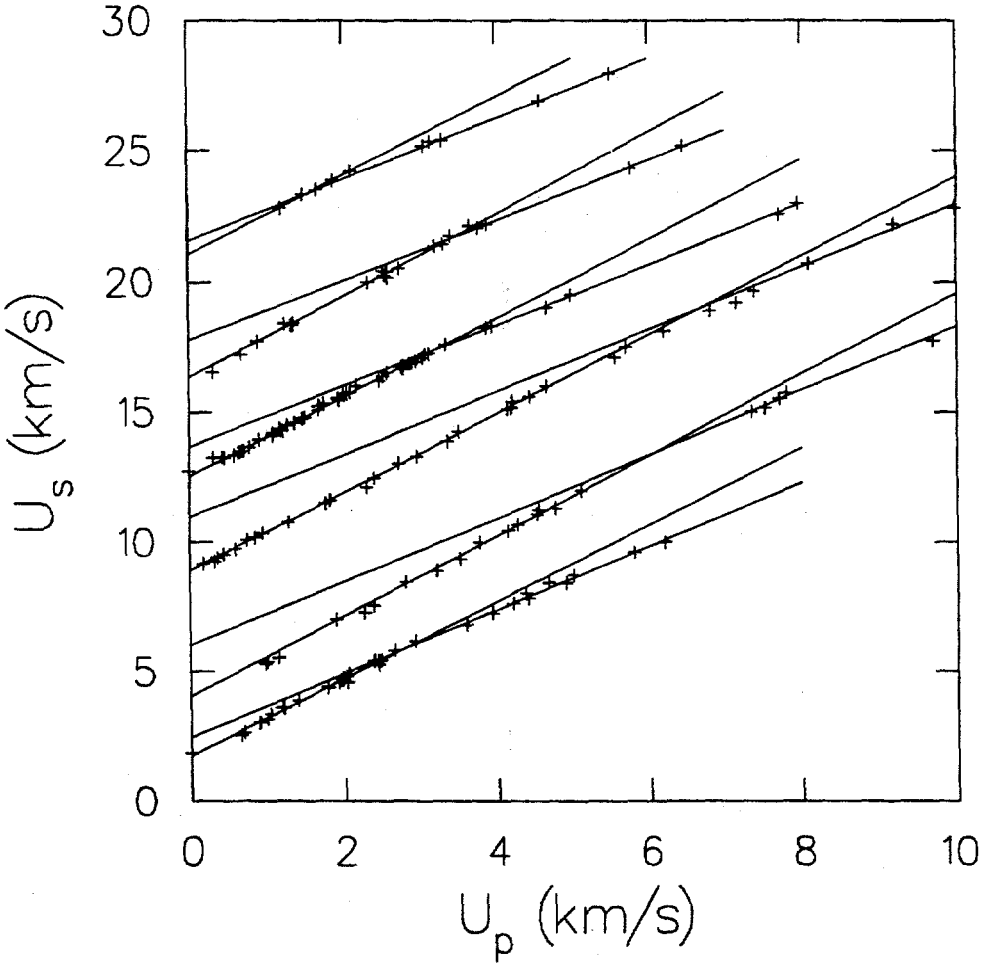

Fig. 4. Bi, Fe, Cu, Sn, Ar, and Xe Hugoniot data from bottom to top. Shifts have been introduced to avoid overlaps.

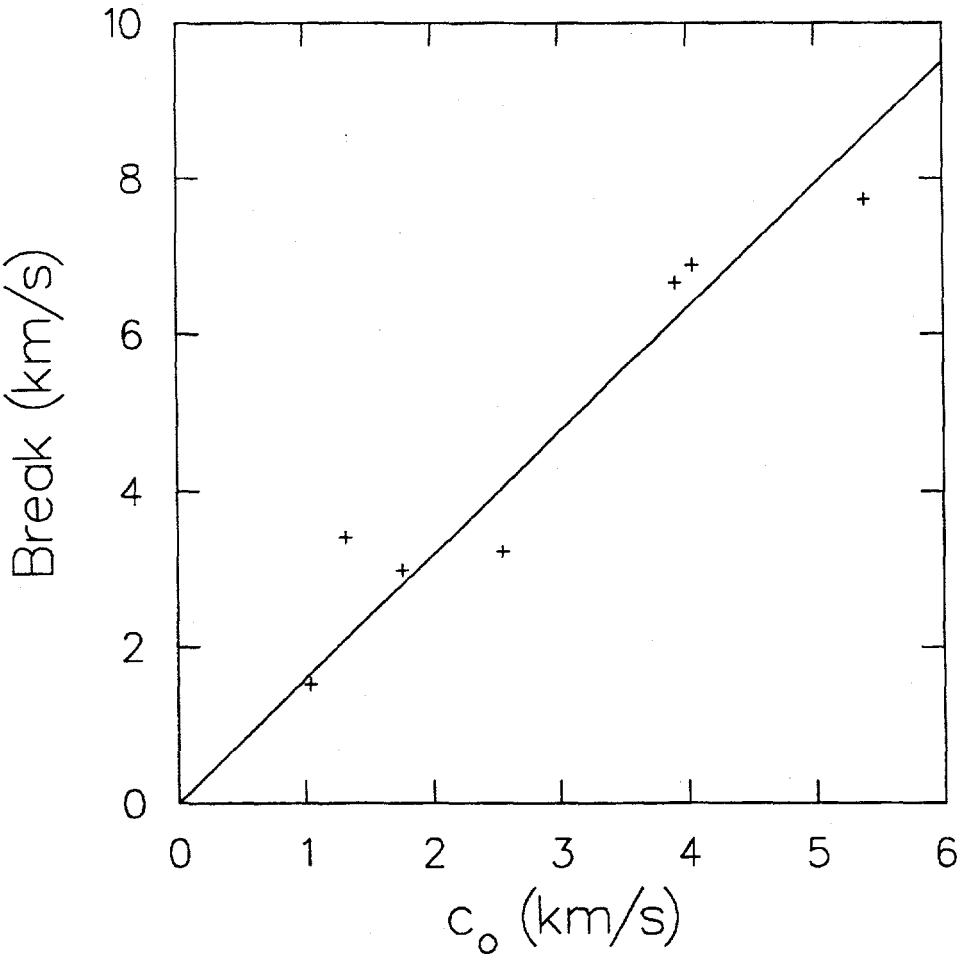

Fig. 5. Breakpoint as a function of c_o.